Cerebral Cortex, November 2016;26: 4136–4147

doi: 10.1093/cercor/bhw225
Advance Access Publication Date: 22 August 2016
Original Article

ORIGINAL ARTICLE

Stimulus-Driven Reorienting Impairs Executive Control of Attention: Evidence for a Common Bottleneck in Anterior Insula

Fynn-Mathis Trautwein, Tania Singer, and Philipp Kanske

Department of Social Neuroscience, Max Planck Institute for Human Cognitive and Brain Sciences, 04103 Leipzig, Germany

Address correspondence to Fynn-Mathis Trautwein, Department of Social Neuroscience, Max Planck Institute for Human Cognitive and Brain Sciences, Stephanstr. 1a, 04103 Leipzig, Germany. Email: trautwein@cbs.mpg.de

Abstract

A classical model of human attention holds that independent neural networks realize stimulus-driven reorienting and executive control of attention. Questioning full independence, the two functions do, however, engage overlapping networks with activations in cingulo-opercular regions such as anterior insula (AI) and a reverse pattern of activation (stimulus-driven reorienting), and deactivation (executive control) in temporoparietal junction (TPJ). To test for independent versus shared neural mechanisms underlying stimulus-driven and executive control of attention, we used fMRI and a task that isolates individual from concurrent demands in both functions. Results revealed super-additive increases of left AI activity and behavioral response costs under concurrent demands, suggesting a common bottleneck for stimulus-driven reorienting and executive control of attention. These increases were mirrored by non-additive decreases of activity in the default mode network (DMN), including posterior TPJ, regions where activity increased with off-task processes. The deactivations in posterior TPJ were spatially separated from stimulus-driven reorienting related activation in anterior TPJ, a differentiation that replicated in task-free resting state. Furthermore, functional connectivity indicated inhibitory coupling between posterior TPJ and AI during concurrent attention demands. These results demonstrate a role of AI in stimulus-driven and executive control of attention that involves down-regulation of internally directed processes in DMN.

Key words: fMRI, functional connectivity, flanker task, spatial cueing, temporoparietal junction

Introduction

For flexible but coherent action in a complex environment, attention must capture important events and single out goal-relevant information. A classical neurocognitive model holds that this is accomplished through two functions—orienting and executive control of attention—which rely on distinct brain networks that can be further decomposed into several sub-networks (Posner and Petersen 1990; Petersen and Posner 2012).

Regarding orienting, a dorsal frontoparietal network consisting of intraparietal sulcus (IPS) and frontal eye fields (FEF) is involved in spatial allocation of attention towards specific stimuli (Kim et al. 1999; Peelen et al. 2004; Molenberghs et al. 2007; Slagter et al. 2007); while ventral frontoparietal areas including temporoparietal junction (TPJ) and inferior frontal gyrus (IFG) are additionally activated whenever a task-relevant stimulus appears outside the current focus of

attention and triggers a reorienting response (Corbetta et al. 2000; Corbetta and Shulman 2002; Kincade et al. 2005; Gillebert et al. 2013; Stoppel et al. 2013; de Haan et al. 2015). Thus, these ventral regions seem to interact with the dorsal frontoparietal network when moving attention from the current focus towards a new source of information in stimulus-driven reorienting of attention (Corbetta et al. 2008; Shulman and Corbetta 2012; Wen et al. 2012).

Regarding executive control, a network involving anterior insula (AI) and dorsal anterior cingulate stretching into medial frontal cortex (dACC) is considered a core system involved in self-regulation, resolution of conflicts between competing information, and focal attention (Botvinick et al. 2004; Rueda et al. 2005; Dosenbach et al. 2008; Craig 2009; Nelson et al. 2010; Kanske and Kotz 2011; van Steenbergen et al. 2015). An important function of this cingulo-opercular network is to allocate resources to external tasks by down-regulating default mode network (DMN) activity and associated internal task-unrelated processes (Wen et al. 2013; Goulden et al. 2014). Furthermore, it also engages a frontoparietal network for fine-grained control adjustments (Dosenbach et al. 2008; Sridharan et al. 2008).

Evidence for independence of orienting and executive control comes from several studies that orthogonally manipulated both functions and found no behavioral interference or interindividual correlation (Fan et al. 2002, 2005; Fuentes and Campoy 2008), non-overlapping neural networks (Fan et al. 2005) and differential brain oscillations (Fan et al. 2007). Note that the only study which explicitly addressed overlap on a neural level (Fan et al. 2005) relied on a sample size of $n = 16$, and it is possible that overlap may be detected in larger samples with higher statistical power (Button et al. 2013; Friston 2013; Ingre 2013; Lindquist et al. 2013). Furthermore, this study did not evaluate interactions on a neural level and assessed orienting and executive control of attention with two distinct, temporally separated events. Specifically, orienting was assessed by comparing responses to spatially informative versus spatially non-informative cues. Under these conditions, executive control of attention (assessed by comparing targets with congruent vs. incongruent flanker stimuli) was not affected by the orienting manipulation. In contrast, orienting can also be assessed through targets appearing at the uncued (vs. cued) location thereby inducing stimulus-driven reorienting of attention towards the target (Corbetta et al. 2000; Gillebert et al. 2013; de Haan et al. 2015). Note that the term "stimulus-driven" is sometimes used in a narrower context of involuntary or "bottom-up" attention shifts (e.g. Serences et al. 2005). These might rely on other mechanisms compared to the reorienting shifts towards a behaviorally relevant target as in the classic reorienting paradigm, which supposedly also involves top-down processing (Kincade et al., 2005). Importantly, in this paradigm the attention shift is elicited by invalidly cued targets and may induce interference if the target also requires executive control of attention. Interestingly, two recent behavioral studies that tested both functions in this way indicate impaired executive control when reorienting of attention is required (Fan et al. 2009; Spagna et al. 2015). While this suggests that shared processes supporting both functions represent a general bottleneck, the neural mechanisms supporting such complex attentional demands are unknown.

Previous research suggests some degree of functional overlap and thus at least two possible origins of interference. Firstly, the frontoparietal network involved in executive control overlaps with the dorsal orienting network (Dosenbach et al. 2008). Secondly, cingulo-opercular regions are also activated by stimulus-driven attentional capture (Corbetta and Shulman 2002; Asplund et al. 2010; Nelson et al. 2010) and have been characterized as salience network, which detects relevant stimuli (Sridharan et al. 2008; Sterzer and Kleinschmidt 2010; Uddin 2015). Thus, frontoparietal and cingulo-opercular networks have both been implicated in executive control and in stimulus-driven reorienting of attention, potentially constituting processing bottlenecks under concurrent attentional demands.

Besides activation overlap, both functions have opposing effects in TPJ, with activation increase for reorienting (Corbetta et al. 2008), but deactivation during controlled attentional processing (Shulman et al. 1997, 2003; Todd et al. 2005; Kubit and Jack 2013). It is debated, whether this pattern reflects a unitary mechanism (Shulman et al. 2007) or separate, but spatially neighboring functions (Kubit and Jack 2013). Supporting a segmentation view, resting state connectivity studies parcellated the TPJ into anterior portions linked with the ventral attention network and posterior portions coupled with default mode and social cognition related areas (Mars et al. 2012; Bzdok et al. 2013; Kanske et al. 2015). Critically, probing whether reorienting related activation and executive control related deactivation can be attributed to such different subregions of TPJ or are spatially non-separable in tension requires simultaneous assessment of the two functions.

Using fMRI, we addressed these questions by combining two standard approaches to induce stimulus-driven reorienting (spatial cueing) and executive control of attention (flanker-target conflict) in a large sample of healthy participants ($n = 282$).

Materials and Methods

Participants

Data were acquired within a large-scale longitudinal study, the ReSource project (for details about recruitment procedure and testing see Singer et al. in press) of which only the baseline measurement time point before intervention is used here. Data was available for 307 out of 332 study participants (missingness due to study dropout: $n = 5$; missingness due to medical or technical issues $n = 20$). Of these, 25 were excluded due to incorrect or poor task performance (error-rate in one of the experimental blocks above 50%; percentage of misses above 12.5%) leaving a sample of 282 healthy participants (mean age = 40 years, SD = 9; 163 female; 258 right-handed). All participants gave written informed consent and the Ethics Committee of the University of Leipzig, Germany approved the study.

Stimuli and Task

To assess executive control and stimulus-driven reorienting of attention, we employed a task that combines a flanker-target conflict (Eriksen and Eriksen 1974) with spatial cueing of the target location (Posner 1980). Similar combination tasks have been employed previously (Greene et al. 2008; Fan et al. 2009; Spagna et al. 2015), however, these involved exogenous cueing (a star appearing at the location of the target) whereas we employed endogenous cues (a central arrow indicating the target location). This is consistent with previous research on the ventral attention network (Corbetta et al. 2000). Details of the task are provided in Figure 1. After a random fixation period (1500, 1700, 2100, 2900, 4500, or 7700 ms), a central arrow cue appeared for 200 ms indicating the position of the target stimulus. After a random interval (200, 500, or 800 ms), five arrows appeared at the cued location (valid cue condition, 80% of the trials) or at the uncued location (invalid cue condition, 20% of

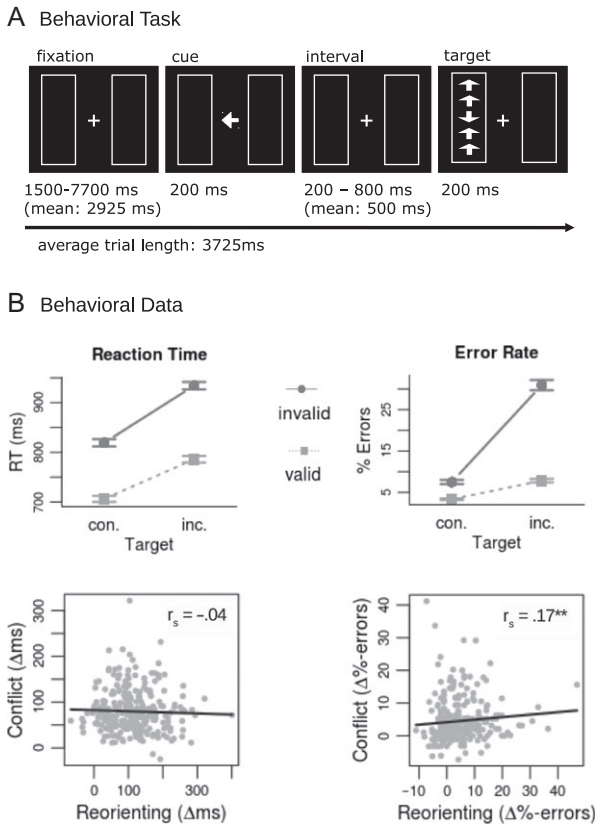

Figure 1. Behavioral task and results (*A*) Example trial of the behavioral task. After a short fixation period, a central cue indicates the correct (validly cued target, depicted) or incorrect location (invalidly cued target) of the forthcoming target stimulus. The direction of the middle arrow indicates the response (left or right button press) and is flanked by arrows pointing in a congruent (con.) or incongruent (inc.) direction. (*B*) Behavioral results. Upper panel: increases in response costs for reaction time and error rate in invalidly cued and incongruent target conditions as well as an interaction effect of both conditions. Lower panel: For reaction time, individual differences in executive control of flanker-target conflict (validly cued incongruent targets – validly cued congruent targets) and stimulus-driven reorienting (invalidly cued congruent targets – validly cued congruent targets) were not correlated; but this correlation was significant for error rates.

the trials). Subjects were instructed to press one of two buttons depending on the direction of the middle arrow (index finger of the right hand for upward arrows and middle finger of the right hand for downward arrows). In half of the trials the middle arrow was flanked by congruent arrows pointing in the same direction (congruent target condition) and in the other half by arrows pointing in the opposite direction (incongruent target condition). Thus the task gives rise to a 2 × 2 factorial design (validly vs. invalidly cued target; congruent vs. incongruent flankers). Overall, 240 trials were presented in a pseudo-randomized order. After each third of the task, two successive questions asked participants to rate task focus ("were you focused on the task?") and task-unrelated thoughts ("did you think of something else?") by moving a marker on a visual analog scale. Rating scales were structured visually by marks ranging from zero to six and were anchored to "not at all" and "entirely". Each rating remained on the screen for eight seconds. Prior to the 16 min. scanning session, participants were familiarized with the task in a short training session (30 trials).

Acquisition of resting state data was done on the same day in a separate scanning session. During the 6 min. run, participants were instructed to focus on a fixation cross in the center of the screen.

MRI Data Acquisition

Brain images were acquired on a 3 T Siemens Verio scanner (Siemens Medical Systems, Erlangen), equipped with a 32-channel head coil. Structural images were acquired using an MPRAGE T1-weighted sequence (TR = 2300 ms; TE = 2.98 ms; TI = 900; flip angle = 9°; 176 sagittal slices; matrix size = 256 × 256; FOV = 256 mm; slice thickness = 1 mm), yielding a final voxel size of 1 × 1 × 1 mm^3. For functional imaging of task and resting state data, a T2*-weighted echo-planar imaging (EPI) sequence was used (TR = 2000 ms; TE = 27 ms, flip angle = 90°). Thirty-seven axial slices were acquired covering the whole brain with a slice thickness of 3 mm, in-plane resolution 3 × 3 mm^2, 1 mm interslice gap, FOV = 210 mm; matrix size 70 × 70. Each run began with three dummy volumes that were discarded, and 490 volumes were acquired during task execution and 190 volumes during rest.

Behavioral Data Analysis

Behavioral data was analyzed using the R software for statistical computing (http://www.R-project.org/). Trials without a response within 200–1700 ms following target onset were discarded. For each participant, mean reaction times (RTs) of correct trials and error rates were calculated for the four conditions of the experimental design. To test for response costs elicited purely by miscued target location and by flanker-target conflict, irrespective of interaction effects, we used paired *t*-tests to compare invalidly with validly cued trials in the congruent flanker condition and incongruent with congruent flanker trials in the valid cue condition. Furthermore, to test for an interaction of cue validity and flanker-target conflict, the condition means were inserted into a repeated measures ANOVA with the factors validity (invalid vs. valid cue) and congruence (incongruent vs. congruent flankers). For correlation analyses, we calculated difference scores for reorienting (invalidly cued congruent targets minus validly cued congruent targets) and conflict resolution (validly cued incongruent minus validly cued congruent targets) for both error rate and reaction time. The invalidly cued incongruent target condition was not used to avoid correlations being driven by the interaction term. Furthermore, we controlled for common variance of both scores potentially induced by the same reference condition (i.e. validly cued congruent target condition, which was used as a control variable) by using partial correlation analysis. All reported associations are based on Spearman's rank correlation coefficient.

fMRI Data Analysis

Preprocessing of Task Data

Images were analyzed using SPM8 (http://www.fil.ion.ucl.ac.uk/spm). All volumes were coregistered to the SPM single-subject canonical EPI image, slice-time corrected and realigned to the mean image volume in order to correct for head motion. Note that no reslicing was applied after initial coregistration, thus the latter did not affect slice-time correction. A high resolution anatomical image of each subject was first coregistered to the SPM single-subject canonical T1 image and then to the average functional image. The transformation matrix obtained by normalizing the anatomical image was then used to normalize

functional images to MNI space. The normalized images (3 mm isotropic voxel) were spatially smoothed with a Gaussian kernel of full-width half-maximum at 8 mm. A high-pass temporal filter with cutoff of 128 s was applied to remove low-frequency drifts from the data.

Assessing Activations of Attention Networks

After preprocessing, statistical analysis was carried out using the general linear model (Friston et al. 1995). Regressors of interest included onsets of the four target conditions (validly and invalidly cued targets with congruent or incongruent flankers) convolved with a canonical hemodynamic response function (HRF). Targets with no or incorrect button presses were omitted. As regressors of no interest, HRF convolved onsets of the cue stimuli and the six motion parameters were included in the design matrix. To further reduce influence of potential noise-artifacts, we used the RobustWLS Toolbox (Diedrichsen and Shadmehr 2005), which down-weights images with higher noise variance through a weighted-least-squares approach.

To assess effects of stimulus-driven reorienting, executive control, and their interaction, contrast images for each cell of the experimental design were calculated for each subject. For random effects analysis (Friston et al. 1999), these were entered into a factorial design with two factors ("cue validity" and "flanker congruence"), with two dependent measurement levels in each factor and unequal variances. Subsequently, the following t-contrasts were defined: Reorienting related activity was assessed by contrasting invalidly cued targets against validly cued targets only within the congruent flanker condition. Vice versa, executive control, that is, incongruently versus congruently flanked targets, was assessed only within the valid cue condition. Common activations within both of these contrasts were evaluated through conjunction analysis by intersecting both individually thresholded contrasts (i.e. testing the conjunction null hypothesis; cf. Nichols et al. 2005). Furthermore, contrasts were defined to test for positive interactions (super-additive effects of invalid cueing and incongruent flankers) and negative interactions (sub-additive effects of both conditions). To qualify the interactions, percent signal change values for each subject were extracted from spheres (radius = 10 mm) around cluster peak voxels using the rfxplot toolbox (Gläscher 2009).

All second-level statistical parametric maps were corrected for multiple comparisons with an extent familywise error (FWE) corrected threshold at $p < 0.05$ (voxel selection threshold at $p < 0.001$). For clusters spanning several anatomical regions, results were assessed at the voxel level with an FWE corrected threshold at $p < 0.05$ (following Woo et al. 2014). For visualization, statistical maps were mapped onto a rendering of the cortical surface using Caret software (Van Essen et al. 2001).

Assessing Task Unrelated Processes

Furthermore, activations due to task unrelated processes were assessed by estimating a separate GLM that included, in addition to the task regressors described above, regressors for on- and off-task periods. To obtain these regressors, the three 10 s intervals prior to the ratings of task focus and task unrelated thoughts were classified based on the composite of both ratings (task focus minus task unrelated thinking) as on- or off-task and convolved with an HRF. The rating scales were structured visually by marks ranging from zero to six. In order to use only probes that could be classified clearly as on- or off-task relative to the subject's own fluctuations, each probe that deviated at least one mark from the individual subject's mean was classified as on- or off-task. This analysis was constrained to those subjects where at least one on-task and one off-task probe was available ($n = 96$). Parameter estimates for on-task versus off-task episodes were contrasted and entered into a one-sample t-test for random effects analysis.

Task-dependent Functional Connectivity Analysis

Condition specific changes in functional connectivity were analyzed using a generalized form of psychophysiological interaction analysis (gPPI), which allows for flexible modeling of multiple experimental conditions (McLaren et al. 2012). The gPPI model included the same task onset and motion parameter regressors as described above. In addition, regressors for a seed region time course extracted from a sphere (radius = 10 mm), and the interaction of each task regressor with the seed region time course were included. For each subject, contrasts for the four target condition by time course interactions were calculated. For the second-level analysis, these were entered into the same full-factorial design as described above.

Analysis of Resting State Data

Resting state data was analyzed with SPM8 and DPARSF (Chao-Gan and Yu-Feng 2010). The first 10 volumes were discarded. The remaining functional scans were slice-time corrected and realigned. T1 images were coregistered to the functional scans and a DARTEL template was created using the averaged T1 images from all subjects. The following nuisance covariates were included: six head motion parameters, the head motion scrubbing regressor, white matter signal, and the CSF signal. Time courses were then band-pass filtered (0.01–0.08 Hz) to reduce the very low-frequency drift, high-frequency respiratory, and cardiac noise.

For functional connectivity calculation, spheres (radius = 10 mm) around task-related peak regions (for details see results section) were defined as seed regions. The averaged time courses were then obtained from the sphere ROIs and voxel-wise correlations computed to generate the functional connectivity maps. The correlation coefficient map was then converted into z maps by Fisher's r-to-z transform to improve normality. These maps, calculated in original space, were normalized into MNI space and re-sampled to 3-mm isotropic voxels as well as smoothed with a 4 mm FWHM kernel. Using random effect analysis, connectivity of different seeds was compared using paired t-tests thresholded at the voxel level at $p < 0.05$ (FWE corrected).

Results

The current study aimed at delineating common and distinct neural contributions as well as the interactive effects of two core attentional functions: stimulus-driven reorienting and executive control of attention. Both functions were independently manipulated in a cued flanker task, allowing to address the following questions: (1) Are there common and distinct neural correlates? (2) Are there non-additive effects on behavior and neural activations, indicating interference in a common bottleneck for both attentional demands? (3) Are both functions independent on the level of interindividual differences, or is there evidence of a common capacity? (4) How are different subregions of the TPJ affected by the tension between stimulus-driven reorienting (activation of TPJ) and executive control demands (deactivation of TPJ)?

Behavioral Data

In order to assess RT and error-rate effects (Fig. 1) of stimulus-driven reorienting and executive control independently from each other, we tested effects of cue validity in the congruent flanker condition and effects of flanker congruency in the valid cue condition. Furthermore, to test for interactive effects of both attention processes, we performed a 2 (cue validity: valid vs. invalid cue) × 2 (flanker congruence: incongruent vs. congruent flanker) repeated-measures ANOVA.

Invalidly compared to validly cued targets led to slower RTs ($t_{(1,281)} = 27.53$, $p < 0.001$). Similarly, RTs were slower in the incongruent compared to the congruent flanker condition ($t_{(1,281)} = 29.55$, $p < 0.001$). Furthermore, a significant interaction effect ($F_{(1,281)} = 47.47$; $p < 0.001$) demonstrated super-additive increases in response costs for the combination of invalid cues and incongruent flankers (consequently, also main effects of the ANOVA were significant for cue validity, $F_{(1,281)} = 973.84$; $p < 0.001$, and flanker congruence, $F_{(1,281)} = 1079.37$; $p < 0.001$). Thus, response costs of simultaneous stimulus-driven reorienting and executive control demands were larger than what would be expected if both processes independently added costs or occurred in parallel. This suggests that both functions depend on a common mechanism that constitutes a processing bottleneck under concurrent demands.

Error-rates showed the same pattern, with higher error-rates for invalidly compared to validly cued targets ($t_{(1,281)} = 9.45$, $p < 0.001$) and more errors in incongruent compared to congruent flanker trials ($t_{(1,281)} = 11.47$, $p < 0.001$). Again super-additive increases in error-rates were indicated by a significant interaction ($F_{(1,281)} = 286.55$; $p < 0.001$) of cue validity (main effect: $F_{(1,281)} = 437.93$; $p < 0.001$) and flanker congruence (main effect: $F_{(1,281)} = 368.50$; $p < 0.001$). Thus, error-rates confirm the results of the RT analysis.

To test independence of interindividual differences in reorienting (i.e. the size of the validity effect in congruent trials) and executive control (i.e. the size of the flanker effect in valid trials) capacities we first checked the intercorrelation (Spearman correlations) of RT scores and error rates. This yielded a significant correlation for executive control ($r_s = 0.26$, $p < 0.001$), while this was not the case for reorienting ($r_s = 0.05$, $p = 0.43$), indicating that reorienting RT scores and error rates are influenced by different sub-processes. For RT scores, correlation analysis of interindividual differences of both capacities (Fig. 1) revealed that executive control and stimulus-driven reorienting were not correlated ($r_s = -0.04$; $p > 0.5$). For error-rates, a positive correlation between both scores was observed ($r_s = 0.17$; $p < 0.01$). This correlation remained practically unchanged ($r_s = 0.16$; $p < 0.01$) when controlling for the common reference condition (i.e. the valid cue congruent flanker condition that is used as a subtraction baseline for both scores) through partial correlation analysis.

fMRI Results

Common and Specific Activations of Stimulus-driven Reorienting and Executive Control

To assess areas involved in stimulus-driven reorienting independently of executive control, we contrasted invalidly with validly cued targets in the congruent condition. Vice versa, executive control of attention was assessed by contrasting incongruent with congruent flanker trials in the valid cue condition. Furthermore, the conjunction of both of these contrasts was evaluated to test for commonalities of both networks (Fig. 2, see Table 1 for a complete list of activated clusters).

Invalidly cued targets induced robust activations in areas previously associated with the ventral orienting network (Corbetta et al. 2008), including left and right TPJ and middle and IFG. Furthermore, parts of the dorsal attention network were activated, such as bilateral intraparietal sulcus and superior frontal gyrus. Further activations involved cingulo-opercular task-control regions with peaks in bilateral anterior insula and dACC (paracingulate gyrus).

Executive control of attention activated areas typically involved in conflict resolution (Nee et al. 2007), such as the cingulo-opercular task-control network as well as in dorsal parietal (IPS) and frontal areas (precentral and middle frontal gyri, near locations often labeled FEF (e.g. Han and Marois 2014).

Conjunction analysis revealed activations in almost all clusters of the main executive control contrast, including AI, dACC, and dorsal frontoparietal areas. Specific activation for executive control of attention was found in inferior temporal gyrus, while stimulus-driven reorienting was associated with specific activations in the TPJ and IFG.

Interactions of Stimulus-driven Reorienting and Executive Control

Having replicated both attention networks as reported in previous research as well as having characterized their considerable overlap, we then tested for positive and negative interactions of cue validity and flanker congruence. Positive interaction could arise from interference of stimulus-driven reorienting and executive control related processes leading to a disproportionate increase of activation. Moreover, negative interactions could arise in regions that are deactivated when task-demands are especially high (Fig. 2, see Table 2 for a complete list of interaction clusters).

A positive interaction was found in left anterior insula, which overlapped with activations in the conjunction analysis. To qualify this interaction effect, we extracted the mean percent signal change within a 10 mm sphere around the peak voxel, which showed a super-additive increase of activation in the condition of joint reorienting and executive control demands (Fig. 2). This pattern mirrors the interaction found in the behavioral analysis, indicating an interference of processes and increased neural resource allocation for invalidly cued incongruent targets in the left anterior insula. Since the conjunction analysis yielded additional areas of functional overlap in frontoparietal and anterior cingulate cortex, areas that have previously been discussed as possible sources of interference (Fan et al. 2009), we also employed a more sensitive ROI approach and extracted the signal from the main peaks of the conjunction analysis. Even though these analyses need to be interpreted carefully as the ROI definition is not fully independent, results notably showed significant super-additive interactions in all cingulo-opercular regions (bilateral AI and dACC, all p-values < 0.04), while none of the interactions for dorsal frontal and parietal conjunction peaks were significant (all p-values > 0.05).

Whole brain analysis of negative interactions yielded clusters in precuneus, as well as left and right posterior TPJ (Fig. 2). Interactions in precuneus and left posterior TPJ were characterized by pronounced decreases of activity for invalidly cued incongruent targets. Thus, these patterns were antagonistic to the super-additive effects in the left anterior insula. Furthermore, right posterior TPJ showed an increase of activity for invalidly cued congruent targets, but a relative decrease for

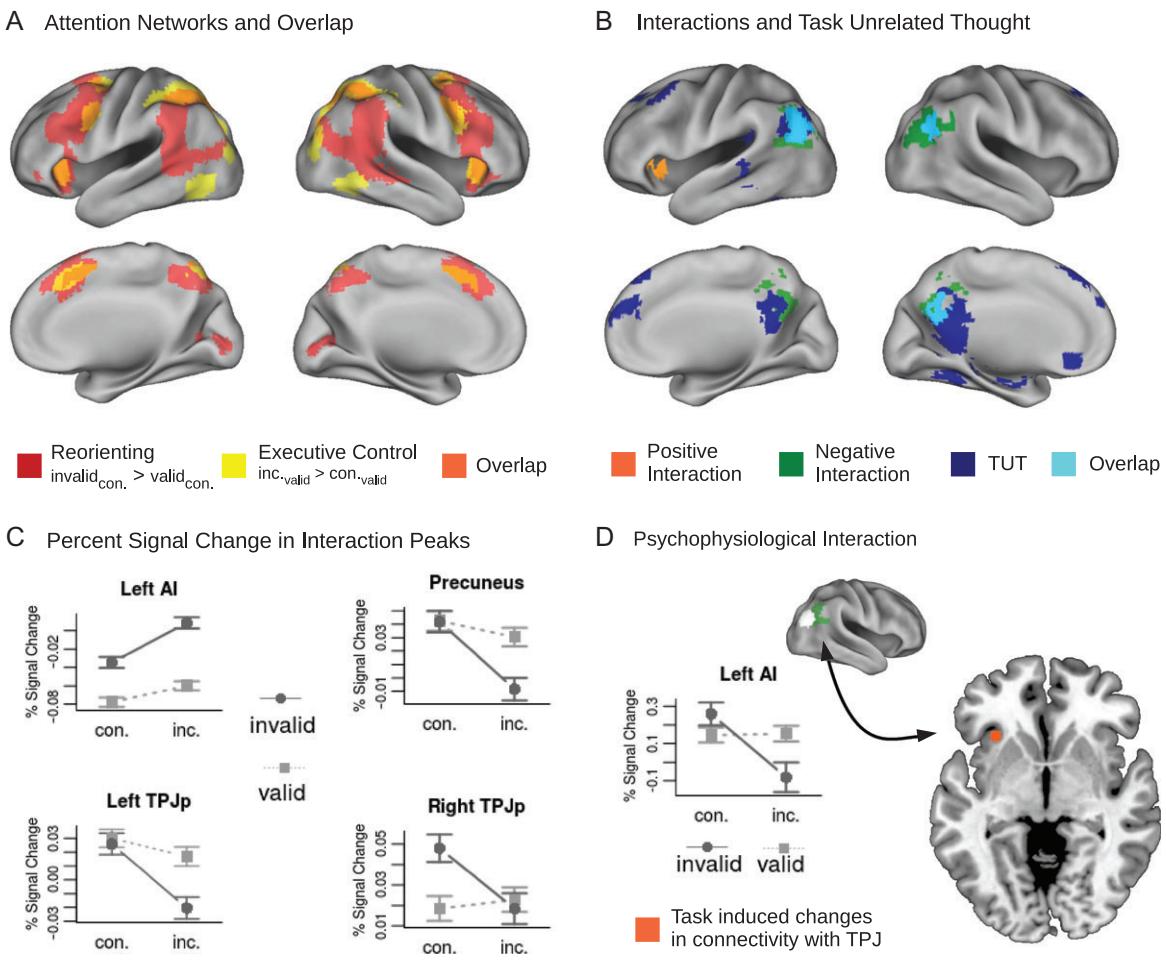

Figure 2. Activation, overlap and interaction of attention networks. (*A*) Activations and overlap of attention networks assessed independently from each other by contrasting invalidly versus validly cued congruent targets (stimulus-driven reorienting, or reorienting) and validly cued incongruent versus congruent targets (executive control). (*B*) A positive interaction of cue (invalid vs. valid) and target condition (incongruent – congruent) was found in left AI, while negative interactions where observed in posterior portions of bilateral TPJ and in Precuneus, overlapping with activations associated with task unrelated thoughts (TUT). (*C*) Percent signal change in interaction peak regions (depicted in B). Left AI shows super-additive increases of activity during reorienting and executive control demands, whereas Precuneus and left TPJ show a reverse pattern of super-additive decreases of activity. Right TPJ shows a response for invalidly cued congruent but not for invalidly cued incongruent targets. (*D*) Psychophysiological interaction analysis yielded negative coupling between right posterior TPJ and left AI during dual reorienting and executive control demands. The graph shows task induced changes in connectivity between posterior TPJ and left AI in the four experimental conditions. *Abbreviations*: TUT = task unrelated thoughts, con. = congruent, inc. = incongruent.

invalidly cued incongruent targets. Thus, this area still showed responses to miscued targets, which were reduced under executive control demands. These interaction clusters in left and right TPJ were located posterior to the reorienting clusters (Fig. 3), stretching from angular gyrus into lateral occipital cortex; and the right cluster overlapped with the posterior portion of a connectivity based parcellation of right TPJ (Bzdok et al. 2013). This pattern is consistent with the view that posterior TPJ is part of the DMN, being deactivated during externally directed attention, while anterior TPJ is coupled with the ventral orienting network (Kubit and Jack 2013). To confirm this differentiation, we directly contrasted activity patterns in anterior and posterior TPJ of the left and right hemisphere. To this end we extracted bold responses for the four peaks and computed the size of the reorienting effect (invalid_congruent – valid_congruent) as well as the size of the interaction effect [(invalid_congruent – valid_congruent) – (invalid_incongruent – valid_incongruent)]. Paired *t*-tests indicated significantly stronger interactions for the posterior peaks (Fig. 3; right hemisphere: $t_{(1,281)} = 2.49$, $p < 0.02$; left hemisphere: $t_{(1,281)} = 2.26$, $p < 0.03$), while reorienting effects were stronger in anterior TPJ (right hemisphere: $t_{(1,281)} = 7.30$, $p < 0.001$; left hemisphere: $t_{(1,281)} = 8.9$, $p < 0.001$). Furthermore, it has been suggested that posterior TPJ also shows a response to miscued targets (as observed in right TPJ), even though it is not involved in the reorienting process itself. Accordingly, activity is suppressed due to the attentional focus induced by the cue, leading to a release of this suppression when the attentional set is broken by a miscued target (Kubit and Jack 2013). To evaluate this hypothesis, we also tested differences in cue related deactivations between anterior and posterior TPJ, which were significant (right hemisphere: $t_{(1,281)} = 9.52$, $p < 0.001$; left hemisphere: $t_{(1,281)} = 11.49$, $p < 0.001$).

Inhibition of Task Unrelated Processes

Previous research has shown that spontaneous task unrelated thought is correlated with activity in the DMN (Mason et al. 2007), which competes for processing resources with attention networks in order to sustain such processes (Anticevic et al. 2012). To test whether the decreases of activity under dual

Table 1. Activation peaks for stimulus-driven reorienting, executive control, and conjunction.

	Hemisphere	MNI coordinates	*t*-Value	Voxels
Stimulus-driven reorienting (invalid congruent > valid congruent)				
Frontal Pole	L	−45, 42, −9	5.29	10
dACC / MFC	L	−6, 15, 51	11.9	3757
Anterior Insula	L	−27, 24, −3	11.74	
Anterior Insula	R	33, 24, −6	11.06	
Middle Frontal Gyrus	L	−39, 6, 36	11.01	
Middle Frontal Gyrus	R	42, 9, 30	10.76	
dACC / MFC	R	9, 18, 48	10.74	
Superior Frontal Gyrus	R	15, 12, 60	8.84	
Inferior Frontal Gyrus	R	51, 21, 6	8.11	
Anterior TPJ	R	54, −45, 24	12.66	3400
Anterior TPJ	L	−54, −48, 36	10.00	
Precuneus	R	9, −54, 48	8.99	
Intraparietal Sulcus	L	−33, −48, 42	8.96	
Middle Temporal Gyrus	R	57, −36, −3	8.48	
Intraparietal Sulcus	R	33, −48, 42	8.37	
Posterior TPJ	R	42, −63, 18	8.33	
Precuneus	L	−9, −57, 51	8.17	
Posterior TPJ	L	−42, −69, 15	7.55	
Occipital Cortex	R	24, −60, 6	5.52	22
Occipital Cortex	R	12, −87, 3	6.79	191.00
Occipital Cortex	L	−9, −90, 0	6.07	
Executive control (valid incongruent > valid congruent)				
Anterior Insula	R	30, 24, 0	8.99	135
Anterior Insula	L	−27, 24, 0	8.79	108
dACC / MFC	R	9, 18, 48	8.09	270
Precentral Gyrus	R	48, 9, 30	8.62	185
Middle Fontal Gyrus	R	27, 6, 54	8.24	215
Middle Fontal Gyrus	L	−27, −3, 51	8.51	345
Precentral Gyrus	L	−45, 3, 33	8.17	
Inferior Temporal Gyrus	R	54, −57, −9	9.38	157
Intraparietal Sulcus	R	24, −60, 48	10.85	1033
Occipital Cortex	R	33, −69, 27	9.19	
Inferior Temporal Gyrus	L	−42, −66, −6	8.89	182
Occipital Cortex	L	−27, −72, 27	9.28	882
Intraparietal Sulcus	L	−18, −63, 48	8.85	
Conjunction: Executive control ∩ Stimulus-driven reorienting				
Anterior Insula	R	30, 24, 0	8.99	133
Anterior Insula	L	−27, 24, 0	8.79	108
dACC / MFC	R	9, 18, 48	8.09	268
Precentral Gyrus	R	48, 9, 30	8.62	166
Middle Fontal Gyrus	R	27, 6, 54	8.11	163
Middle Fontal Gyrus	L	−27, 0, 51	8.49	270
Precentral Gyrus	L	−45, 3, 33	8.17	
Intraparietal Sulcus	L	−36, −45, 45	8.06	479
Intraparietal Sulcus	R	33, −48, 45	8.18	391
Occipital Cortex	R	39, −72, 27	7.46	70

Notes: Activations were assessed at the voxel level with an FWE corrected threshold at $p < 0.05$. All clusters exceeding an extent of $k < 5$ voxels are reported. Clusters are ordered from anterior to posterior. Rows without voxel count refer to sub-peaks within larger clusters; the main peak and voxel count of these clusters is always provided as a first row, and sub-peaks in subsequent rows.

attentional demand might be related to inhibition of such processes, we probed for task unrelated thoughts during the task and used these ratings as parametric modulators of the pre-rating epochs. This analysis yielded regions typically implicated in the DMN (Fig. 2). Arguing for inhibition of task unrelated processes during combined reorienting and executive control of attention, the clusters overlapped with negative interactions in bilateral TPJ and precuneus.

Table 2. Activation peaks for positive and negative interactions.

	Hemisphere	MNI coordinates	*t*-Value	Voxels
Positive interaction				
Anterior Insula	L	−30, 27, 6	4.19	72.00
Negative interaction				
Precuneus	R	6, −57, 33	4.41	308
Posterior TPJ	R	45, −69, 27	4.60	283
Posterior TPJ	L	−42, −69, 33	4.43	309

Notes: Activations were assessed at an extent familywise error (FWE) corrected threshold of $p < 0.05$ (voxel selection threshold at $p < 0.001$). Clusters are ordered from anterior to posterior.

Task-dependent Functional Connectivity of Posterior TPJ

Having shown a potential explanation of the non-additive deactivations—suppression of task unrelated processes—we were interested whether the source of such suppression would be overshooting attentional demands in left anterior insula. To this end, we assessed task-dependent changes in functional connectivity by means of generalized psychophysiological interaction analysis (gPPI; McLaren et al. 2012). Specifically, we tested for correlations between the interaction peak in right TPJ and voxels that showed non-additive positive effects of reorienting and executive control. To this end, we entered the first-level PPI contrasts of the four conditions into a full-factorial design, and tested for negative interactions within a mask defined by the positive interaction contrast. This analysis yielded a significant cluster in left anterior insula ($x = -30$, $y = 24$, $z = -6$; $t = 3.4$; small volume correction, Fig. 2). Thus, connectivity between posterior TPJ and left AI changed for the combination of invalid cues and incongruent flankers. Extracted values indicated that there was increased positive connectivity for the invalidly cued congruent target, but negative coupling for the invalidly cued incongruent target.

Differential Resting State Connectivity of TPJ Subregions

Based on resting state connectivity and metanalytic clustering, previous research has differentiated the TPJ into at least two subregions; a posterior part showing connectivity with the DMN, and an anterior part showing connectivity with the ventral orienting network (Mars et al. 2012; Bzdok et al. 2013). This raises the question as to whether the current task-based differentiation within TPJ conforms to previous resting state connectivity based parcellations. We therefore analyzed resting state data from the same individuals as in the task analysis (Fig. 3). Relative to the posterior interaction peak, the anterior reorienting peak showed increased connectivity with anterior cingulate and medial frontal cortex, bilateral anterior insula, inferior and middle frontal gyrus. In contrast, the interaction peak was associated with increased connectivity to posterior cingulate and precuneus, hippocampus, and medial frontal cortex. Thus, consistent with previous literature, the functional peak activations for reorienting and the interaction effect were part of corresponding ventral attention and DMN resting-state networks.

Discussion

Describing the architecture of human attentional systems has been one of the main challenges tackled by cognitive

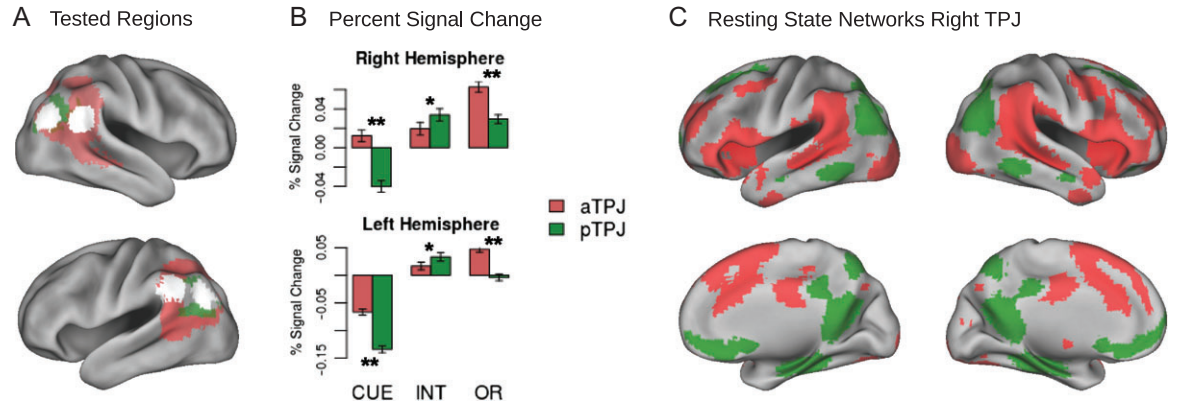

Figure 3. Functional differentiation of subregions in TPJ. (*A*) White areas depict spheres in anterior TPJ and posterior TPJ around peak activations of reorienting contrast (red) and negative interaction contrast (green). These spheres were used to extract percent signal change (shown in *B*) and activation time courses for connectivity analysis (shown in *C*, only done for right TPJ). (*B*) Deactivation induced by orienting cues (CUE) and interaction of dual attentional demands (INT) were stronger in posterior compared to anterior TPJ, while stimulus-driven reorienting (OR) elicited stronger activations in anterior TPJ. (*C*) Resting state functional connectivity networks of anterior TPJ (red) and posterior TPJ (green) contrasted against each other.

neuroscience. Previous research has described two main attention systems that supposedly rely on several independent neural networks: one system spatially orienting attention towards relevant stimuli and another system exerting executive control (Posner and Petersen 1990; Petersen and Posner 2012). Here, we put the assumption of independence of the two systems to test by assessing behavioral responses and neural activations in a task that concurrently demands both functions through spatial cueing and flanker-target conflict. Results replicate cingulo-opercular and frontoparietal networks for executive control as well as dorsal and ventral orienting networks. However, in contrast to the assumption of independence, we provide evidence for a shared mechanism in AI, leading to interferences (i.e. lower processing efficiency) in situations that concurrently demand stimulus-driven reorienting and executive control of attention. This was evidenced by super-additive increases in response costs and left AI activity for the combination of both attentional processes. Deactivations due to dual attentional demands in posterior TPJ and precuneus—regions also activated by task unrelated thought—further indicated reliance on common mechanisms. Task-dependent functional connectivity analysis revealed negative coupling between regions showing non-additive deactivation (posterior TPJ) and activation (left AI), suggesting that task unrelated processes might be increasingly suppressed with higher and concurrent attentional demands. This finding also revealed a spatial differentiation of processes within TPJ, with suppression of posterior TPJ by attentional demands, and activation of anterior TPJ during reorienting—a task-based differentiation which we confirmed with resting-state functional connectivity.

Resource Competition of Attention Systems

Previous research has mainly characterized executive control and stimulus-driven reorienting of attention as two independent systems (Fan et al. 2005; Petersen and Posner 2012). However, more recent behavioral studies tailored to reveal interactions between both systems found evidence for interference (Fan et al. 2009; Spagna et al. 2015). Consistent with these studies, we found that response costs resulting from incongruent flankers surrounding the target stimulus were enhanced when targets were preceded by invalid cues. This condition induces reorienting—attention is moved from the previously indicated field to the location of target appearance—while it requires executive control in order to resolve the flanker-target conflict. Thus, in a situation with concurrent stimulus-driven reorienting and executive control requirements, both processes interfere with each other, pointing towards a shared mechanism or a common "bottleneck." Furthermore, we tested whether reorienting and executive control are independent on the level of interindividual differences. In agreement with other studies (Fan et al. 2002, 2005; Fossella et al. 2002; Greene et al. 2008; Spagna et al. 2015), reaction time scores of both capacities were not correlated. However, we observed a significant positive correlation for error rates. To our knowledge, correlational analyses in error-rates have only been reported by Fan et al. (2007), who also found a positive correlation. Note that the correlation remained significant when controlling for variation induced by the common reference condition of both scores. Considering that error rates also showed a stronger interaction effect in the within subject analysis (effect size η^2 of interaction term: 0.13 for errors vs. 0.006 for RT) and thus potentially have a higher susceptibility to the performance limiting bottleneck, this might indeed indicate that both functions are limited by a common individual capacity. The lacking correlation between RT scores of both capacities might be further explained by the fact that, for reorienting, there was no correlation between RT scores and error rates. Thus interindividual differences in both of these indices might be influenced by different sub-processes contributing to stimulus-driven reorienting. Future research might provide a more fine-grained understanding of these different sub-processes by modeling cognitive processes that account for the RT and accuracy distributions across trials (e.g. Voss et al., 2013).

Previously, two potential origins of interference have been proposed (Fan et al. 2009): (1) the dorsal orienting network, which might not only be recruited by orienting but also to filter out incongruent flanker stimuli and (2) cingulo-opercular areas which are not only activated during executive control, but also by task relevant events (Uddin 2015). Consistent with both possibilities, overlapping activations were found in frontoparietal and cingulo-opercular regions. Importantly, however, whole brain analysis yielded non-additive increases of activity and hence evidence for interference of processes only in left AI. Moreover, a more sensitive region of interest analysis revealed the same interaction pattern in right AI and dACC, while there

were no interactions in any of the dorsal frontoparietal areas. In line with these results, recent accounts have attributed central functions to cingulo-opercular regions within the domain of attention. These include focal attention (Nelson et al. 2010), a unified bottleneck of perception and response related attention (Tombu et al. 2011), stimulus- and task-driven alertness (Sterzer and Kleinschmidt 2010), and salience-based regulation of executive regions and the DMN in order to allocate processing resources to relevant stimuli (Sridharan et al. 2008; Uddin 2015; Cai et al. 2016). Furthermore, a recent study (Han and Marois 2014) indicated that AI might in fact be more central to the attentional reorienting process then temporoparietal areas, which could rather relate to subsequent stimulus evaluation processes (Geng and Vossel 2013).

Several sub-processes such as salience or error processing, contingent capture (Folk 1992), target detection (Kubit and Jack 2013), and disengagement and shifting of attention (Posner et al. 1984) might contribute to the reorienting process as implemented in the current study—which limits conclusions about the precise mechanism that interfered with executive control of attention. It has been shown that the ventral attention network is not activated during attentional capture driven purely by perceptual saliency (Kincade et al. 2005), but during reorienting to non-target stimuli with task relevant features (Serences et al. 2005) and targets with low salience (Indovina and Macaluso 2007). Thus it can be assumed that the involved mechanism is not a pure bottom-up process, but also involves top-down modulations that filter for task relevant features (Corbetta et al. 2008). Furthermore, post-perceptual processes such as contextual updating and adjustment of expectations might also be involved (Geng and Vossel 2013). This also implies that the present results do not rule out that attentional capture purely driven by perceptual features might work independently from executive control of attention. The fact that previous studies assessing orienting with spatially informative versus non-informative cues did not find an interaction with executive control (Fan et al. 2002, 2005; Fuentes and Campoy 2008)—but the present and other studies inducing reorienting through invalid cues did (Fan et al. 2009; Spagna et al. 2015)—might further clarify the mechanism involved in the interaction. One process classically thought to be present only in reorienting (induced by invalid cueing) is disengagement of attentional focus from the previous target location (Posner et al. 1984). Thus a potential explanation of these discrepancies is that inhibitory mechanisms involved in disengaging attention during reorienting create interference. This is plausible because inhibitory mechanisms are also involved in conflict resolution (Nee et al. 2007) and agrees with the locus of neural interactions in cingulo-opercular, but not in dorsal frontoparietal regions. Furthermore, the low temporal resolution of fMRI data limits conclusions about the exact time course dynamics of processes involved in stimulus-driven reorienting and executive control of attention. While both are elicited by the appearance of the same stimulus (in the case of invalidly cued incongruent targets), it is possible that the conflict processing is only engaged when attention has at least partially reoriented. Future studies using methods with higher temporal resolution could reveal to which extent overlapping dynamics of the two processes result in the behavioral interaction.

Nevertheless, the present results are particularly supportive of the view that the mechanism implemented in AI is responsible for suppression of DMN activity, which is considered a mechanism to reduce interference from internally focused processes, such as task unrelated thought, during externally focused attention (Anticevic et al. 2012; Wen et al. 2013). If simultaneous executive control and stimulus-driven reorienting of attention causes overshoot in processing demands, this might also induce increased down-regulation of DMN activity. In agreement with such an antagonistic relationship, we observed non-additive decreases of activity for concurrent reorienting and conflict resolution demands in bilateral posterior TPJ and in precuneus, areas linked to the DMN (Gusnard and Raichle 2001). Indicating that these deactivations indeed reflect inhibition of internally focused cognition, the negative interaction effects overlapped with activations induced by task unrelated thought. Furthermore, to directly characterize the relationship between these non-additive decreases and increases of activity, we investigated task-dependent functional connectivity of the main deactivation peak in posterior right TPJ, which yielded negative coupling between this region and left AI under combined reorienting and conflict resolution demands. Consistent with its role as a causal hub between inwardly and outwardly directed processing systems (Menon and Uddin 2010; Kanske et al. 2016), this suggests that AI may down-regulate distracting processes in the DMN when capacity limits are reached.

Functional Differentiations in TPJ

The negative interaction effect indicating down-regulation of posterior TPJ during concurrent attentional demands is also informative in relation to the debated question of segregated functions versus a unitary mechanism within TPJ (Cabeza et al. 2012; Nelson et al. 2012). Specifically, this interaction was stronger in posterior TPJ compared to anterior TPJ. Vice versa, reorienting preferentially activated anterior TPJ. This double dissociation provides direct evidence that anterior TPJ is recruited in the reorienting process, while posterior TPJ is deactivated during high attentional task demands. This dissociation is consistent with resting state functional connectivity studies and meta-analytic evidence, which situates posterior TPJ in a network activated during social cognition and mind-wandering, but deactivated by a wide range of attention tasks; while linking anterior TPJ with the ventral attention network (Shulman et al. 1997; Fox et al. 2006; Bzdok et al. 2013; Carter and Huettel 2013; Kanske et al. 2015; Krall et al. 2015).

In order to confirm this differentiation and relate it to prior parcellation studies, we analyzed resting-state functional connectivity. Consistent with previous research (Yeo and Krienen 2011), results yielded coupling of posterior TPJ with typical DMN regions including medial PFC, precuneus, and hippocampus, while anterior TPJ was coupled with regions of cingulo-opercular and ventral attention networks including AI, dACC, and inferior and middle frontal gyri.

It is important to note that right posterior TPJ also showed an increase of activity for invalid congruent targets. This pattern might be explained by several factors: Firstly, the increase might reflect release of suppression, which was suggested by Kubit and Jack (2013) to account for the meta-analytic finding that reorienting partially overlapped with a “pure” social cognition cluster in posterior TPJ, but also with a “pure” anterior target detection cluster. Accordingly, TPJ activations in the reorienting paradigm are the result of two distinct but spatially neighboring mechanisms: Posterior TPJ is suppressed when attention is focused in response to the cue, and this suppression is released when the attentional set is broken by the miscued target. In contrast, anterior TPJ is activated due to target detection. Beyond the double dissociation discussed above, this

view is supported by the fact that the cue mainly caused deactivations in posterior TPJ. Furthermore, if suppression is maintained for invalidly cued incongruent targets due to executive control demands, this would explain why there is a response (i.e., release of suppression) only for invalidly cued congruent targets. A second factor that might contribute to the interaction pattern in right posterior TPJ is spatial "blurring" of reorienting and suppression effects due to methodological noise (e.g., limited spatial resolution), or true overlap of related neural populations. Furthermore, the fact that left posterior TPJ mainly showed deactivations for invalid incongruent targets is consistent with previously shown right hemispheric dominance in stimulus-driven reorienting (Corbetta et al. 2008; Kubit and Jack 2013).

In sum, the current results provide evidence that stimulus-driven reorienting and executive control of attention rely on a shared mechanism in left AI and potentially other cingulo-opercular regions, leading to behavioral interference and inhibition of task unrelated processes in the DMN. This argues for a central role of AI within both types of attention, leading to additional down-regulation of internally directed processes when capacity limits are reached. Furthermore, results support a functional segregation of TPJ into an anterior part responding to unexpected, task-relevant stimuli, and a posterior part that is suppressed during high attentional task demands.

This characterization of the overlap, differentiation, and interaction of attentional functions bears relevance for our understanding of a range of clinical conditions (Broyd et al. 2009), and can also contribute to the future development of interventions that support self-regulation of attention in clinical and healthy populations (Lutz et al. 2008; Malinowski 2013; Tang and Posner 2014).

Funding

European Research Council (ERC) under the European Community's Seventh Framework Programme (205557 to T.S.).

Notes

We are grateful to the Department of Social Neurosciences for their support with the ReSource project, to Manuela Hofmann, Sylvia Neubert and Nicole Pampus for their help with data acquisition, and to Shameem Wagner for proofreading the manuscript. *Conflict of Interest:* None declared.

References

Anticevic A, Cole MW, Murray JD, Corlett PR, Wang X-J, Krystal JH. 2012. The role of default network deactivation in cognition and disease. Trends Cogn Sci. 16:584–592.

Asplund CL, Todd JJ, Snyder AP, Marois R. 2010. A central role for the lateral prefrontal cortex in goal-directed and stimulus-driven attention. Nat Neurosci. 13:507–512.

Botvinick MM, Cohen JD, Carter CS. 2004. Conflict monitoring and anterior cingulate cortex: an update. Trends Cogn Sci. 8:539–546.

Broyd SJ, Demanuele C, Debener S, Helps SK, James CJ, Sonuga-Barke EJS. 2009. Default-mode brain dysfunction in mental disorders: a systematic review. Neurosci Biobehav Rev. 33:279–296.

Button KS, Ioannidis JPA, Mokrysz C, Nosek BA, Flint J, Robinson ESJ, Munafò MR. 2013. Power failure: why small sample size undermines the reliability of neuroscience. Nat Rev Neurosci. 14:365–376.

Bzdok D, Langner R, Schilbach L, Jakobs O, Roski C, Caspers S, Laird AR, Fox PT, Zilles K, Eickhoff SB. 2013. Characterization of the temporo-parietal junction by combining data-driven parcellation, complementary connectivity analyses, and functional decoding. NeuroImage. 81:381–392.

Cabeza R, Ciaramelli E, Moscovitch M. 2012. Cognitive contributions of the ventral parietal cortex: an integrative theoretical account. Trends Cogn Sci. 16:338–352.

Cabeza R, Ciaramelli E, Moscovitch M. 2012. Response to Nelson et al.: ventral parietal subdivisions are not incompatible with an overarching function. Trends Cogn Sci. 16:400–401.

Cai W, Chen T, Ryali S, Kochalka J, Li C-SR, Menon V. 2016. Causal interactions within a frontal-cingulate-parietal network during cognitive control: convergent evidence from a multisite–multitask investigation. Cereb Cortex. 26:2140–2153.

Carter RM, Huettel SA. 2013. A nexus model of the temporal–parietal junction. Trends Cogn Sci. 17:328–336.

Chao-Gan Y, Yu-Feng Z. 2010. DPARSF: a MATLAB Toolbox for "Pipeline" data analysis of resting-state fMRI. Front Syst Neuroscience. 4:13–13.

Chen Q, Weidner R, Vossel S, Weiss PH, Fink GR. 2012. Neural mechanisms of attentional reorienting in three-dimensional space. J Neurosci. 32:13352–13362.

Corbetta M, Kincade JM, Ollinger JM, McAvoy MP, Shulman GL. 2000. Voluntary orienting is dissociated from target detection in human posterior parietal cortex. Nat Neurosci. 3:292–297.

Corbetta M, Patel G, Shulman GL. 2008. The reorienting system of the human brain: from environment to theory of mind. Neuron. 58:306–324.

Corbetta M, Shulman GL. 2002. Control of goal-directed and stimulus-driven attention in the brain. Nat Rev Neurosci. 3:201–215.

Craig ADB. 2009. How do you feel–now? The anterior insula and human awareness. Nat Rev Neurosci. 10:59–70.

de Haan, B, Bither, M, Brauer, A, Karnath, H-O. 2015. Neural correlates of spatial attention and target detection in a multi-target environmentCereb Cortex. 25:2321–2331.

Diedrichsen J, Shadmehr R. 2005. Detecting and adjusting for artifacts in fMRI time series data. NeuroImage. 27:624–634.

Dosenbach NUF, Fair DA, Cohen AL, Schlaggar BL, Petersen SE. 2008. A dual-networks architecture of top-down control. Trends Cogn Sci. 12:99–105.

Eriksen BA, Eriksen CW. 1974. Effects of noise letters upon the identification of a target letter in a nonsearch task. Percept Psychophys. 16:143–149.

Fan J, Byrne J, Worden MS, Guise KG, McCandliss BD, Fossella J, Posner MI. 2007. The relation of brain oscillations to attentional networks. J Neurosci. 27:6197–6206.

Fan J, Gu X, Guise KG, Liu X, Fossella J, Wang H, Posner MI. 2009. Testing the behavioral interaction and integration of attentional networks. Brain Cogn. 70:209–220.

Fan J, McCandliss BD, Fossella J, Flombaum JI, Posner MI. 2005. The activation of attentional networks. NeuroImage. 26:471–479.

Fan J, McCandliss BD, Sommer T, Raz A, Posner MI. 2002. Testing the efficiency and independence of attentional networks. J Cogn Neurosci. 14:340–347.

Folk CL, Remington RW, Johnston JC. 1992. Involuntary covert orienting is contingent on attentional control settings. J Exp Psychol Human. 18:1030–1044.

Fossella J, Sommer T, Fan J, Wu Y, Swanson JM, Pfaff DW, Posner MI. 2002. Assessing the molecular genetics of attention networks. BMC Neuroscience. 3:14–14.

Fox MD, Corbetta M, Snyder AZ, Vincent JL, Raichle ME. 2006. Spontaneous neuronal activity distinguishes human dorsal and ventral attention systems. PNAS. 103:10046–10051.

Friston KJ. 2013. Sample size and the fallacies of classical inference. Neuroimage. 81:503–504.

Friston KJ, Holmes AP, Price CJ, Büchel C, Worsley KJ. 1999. Multisubject fMRI studies and conjunction analyses. Neuroimage. 396:385–396.

Friston KJ, Holmes AP, Worsley KJ, Poline JP, Frith CD, Fackowiak RSJ. 1995. Statistical parametric maps in functional imaging: a general linear approach. Hum Brain Mapp. 2:189–210.

Fuentes LJ, Campoy G. 2008. The time course of alerting effect over orienting in the attention network test. Exp Brain Res. 185:667–672.

Geng JJ, Vossel S. 2013. Re-evaluating the role of TPJ in attentional control: Contextual updating? Neurosci and Biobehav R. 37:2608–2620.

Gillebert CR, Mantini D, Peeters R, Dupont P, Vandenberghe R. 2013. Cytoarchitectonic mapping of attentional selection and reorienting in parietal cortex. NeuroImage. 67:257–272.

Gläscher J. 2009. Visualization of group inference data in functional neuroimaging. Neuroinformatics. 7:73–82.

Goulden N, Khusnulina A, Davis NJ, Bracewell RM, Bokde AL, McNulty JP, Mullins PG. 2014. The salience network is responsible for switching between the default mode network and the central executive network: replication from DCM. NeuroImage. 99:180–190.

Greene DJ, Barnea A, Herzberg K, Rassis A, Neta M, Raz A, Zaidel E. 2008. Measuring attention in the hemispheres: the lateralized attention network test (LANT). Brain Cogn. 66:21–31.

Gusnard DA, Raichle ME. 2001. Searching for a baseline: functional imaging and the resting human brain. Nat Rev Neurosci. 2:685–694.

Han SW, Marois R. 2014. Functional fractionation of the stimulus-driven attention network. J Neurosci. 34:6958–6969.

Indovina I, Macaluso E. 2007. Dissociation of stimulus relevance and saliency factors during shifts of visuospatial attention. Cereb Cortex. 17:1701–1711.

Ingre M. 2013. Why small low-powered studies are worse than large high-powered studies and how to protect against "trivial" findings in research: comment on Friston (2012). Neuroimage. 81:496–498.

Kanske P, Böckler A, Trautwein F-M, Singer T. 2015. Dissecting the social brain: introducing the EmpaToM to reveal distinct neural networks and brain–behavior relations for empathy and Theory of Mind. NeuroImage. 122:6–19.

Kanske P, Böckler A, Trautwein F-M, Parianen Lesemann FH, Singer T. 2016. Are strong empathizers better mentalizers? Evidence for independence and interaction between the routes of social cognition. Soc Cogn Affect Neurosci. Advance Access published April 28, 2016, doi:10.1093/scan/nsw052.

Kanske P, Kotz SA. 2011. Emotion speeds up conflict resolution: a new role for the ventral anterior cingulate cortex?. Cereb Cortex. 21:911–919.

Kim YH, Gitelman DR, Nobre AC, Parrish TB, LaBar KS, Mesulam MM. 1999. The large-scale neural network for spatial attention displays multifunctional overlap but differential asymmetry. NeuroImage. 9:269–277.

Kincade JM, Abrams RA, Astafiev SV, Shulman GL, Corbetta M. 2005. An event-related functional magnetic resonance imaging study of voluntary and stimulus-driven orienting of attention. J Neurosci. 25:4593–4604.

Krall SC, Rottschy C, Oberwelland E, Bzdok D, Fox PT, Eickhoff SB, Fink GR, Konrad K. 2015. The role of the right temporoparietal junction in attention and social interaction as revealed by ALE meta-analysis. Brain Struct Funct. 220:587–604.

Kubit B, Jack AI. 2013. Rethinking the role of the rTPJ in attention and social cognition in light of the opposing domains hypothesis: findings from an ALE-based meta-analysis and resting-state functional connectivity. Front Hum Neurosci. 7:1–18.

Lindquist MA, Caffo B, Crainiceanu C. 2013. Ironing out the statistical wrinkles in "ten ironic rules". NeuroImage. 81:499–502.

Lutz A, Slagter HA, Dunne JD, Davidson RJ. 2008. Attention regulation and monitoring in meditation. Trends Cogn Sci. 12:163–169.

Malinowski P. 2013. Neural mechanisms of attentional control in mindfulness meditation. Front Neurosci. 7:1–11.

Mars RB, Sallet J, Schüffelgen U, Jbabdi S, Toni I, Rushworth MFS. 2012. Connectivity-based subdivisions of the human right "temporoparietal junction area": evidence for different areas participating in different cortical networks. Cereb Cortex. 22:1894–1903.

Mason MF, Norton MI, Van Horn JD, Wegner DM, Grafton ST, Macrae CN. 2007. Wandering minds: the default network and stimulus-independent thought. Science. 315:393–395.

McLaren DG, Ries ML, Xu G, Johnson SC. 2012. A generalized form of context-dependent psychophysiological interactions (gPPI): a comparison to standard approaches. NeuroImage. 61:1277–1286.

Menon V, Uddin LQ. 2010. Saliency, switching, attention and control: a network model of insula function. Brain Struct Funct. 214:655–667.

Molenberghs P, Mesulam MM, Peeters R, Vandenberghe RRC. 2007. Remapping attentional priorities: differential contribution of superior parietal lobule and intraparietal sulcus. Cereb Cortex. 17:2703–2712.

Nee DE, Wager TD, Jonides J. 2007. Interference resolution: insights from a meta-analysis of neuroimaging tasks. Cogn Affect Behav Neurosci. 7:1–17.

Nelson SM, Dosenbach NUF, Cohen AL, Wheeler ME, Schlaggar BL, Petersen SE. 2010. Role of the anterior insula in task-level control and focal attention. Brain Struct Funct. 214:669–680.

Nelson SM, McDermott KB, Petersen SE. 2012. In favor of a "fractionation" view of ventral parietal cortex: comment on Cabeza et al. Trends Cogn Sci. 16:399–400.

Nichols T, Brett M, Andersson J, Wager T, Poline J-B. 2005. Valid conjunction inference with the minimum statistic. NeuroImage. 25:653–660.

Peelen MV, Heslenfeld DJ, Theeuwes J. 2004. Endogenous and exogenous attention shifts are mediated by the same large-scale neural network. Neuroimage. 22:822–830.

Petersen SE, Posner MI. 2012. The attention system of the human brain: 20 years after. Annu Rev Neurosci. 35:73–89.

Posner MI. 1980. Orienting of attention. Q J Exp Psychol. 32:3–25.

Posner MI, Petersen SE. 1990. The attention system of the human brain. Annu Rev Neurosci. 13:25–42.

Posner MI, Walker JA, Friedrich FJ, Rafal RD. 1984. Effects of parietal injury on covert orienting of attention. J Neurosci. 4:1863–1874.

Rueda MR, Rothbart MK, McCandliss BD, Saccomanno L, Posner MI. 2005. Training, maturation, and genetic influences on

the development of executive attention. Proc Natl Acad Sci USA. 102:14931–14936.

Serences JT, Shomstein S, Leber AB, Golay X, Egeth HE, Yantis S. 2005. Coordination of voluntary and stimulus-driven attentional control in human cortex. Psychol Sci. 16: 114–122.

Shulman GL, Astafiev SV, McAvoy MP, d'Avossa G, Corbetta M. 2007. Right TPJ deactivation during visual search: functional significance and support for a filter hypothesis. Cereb Cortex. 17:2625–2633.

Shulman GL, Corbetta M. 2012.Two attentional networks: identification and function within a larger cognitive architecture. In: Posner MI, editor. Cognitive neuroscience of attention. The Guilford Press, New York, 2nd ed. p. 113–128.

Shulman GL, Fiez JA, Corbetta M. 1997. Common blood flow changes across visual tasks: II. Decreases in cerebral cortex. J Cogn Neurosci. 9:648–663.

Shulman GL, McAvoy MP, Cowan MC, Astafiev SV, Tansy AP, d'Avossa G, Corbetta M. 2003. Quantitative analysis of attention and detection signals during visual search. J Neurophysiol. 90:3384–3397.

Singer T, Kok BE, Bornemann B, Zurborg S, Bolz M, Bochow CA. in press. The ReSource Project. Background, design, samples, and measurements. 2nd ed. Leipzig: Max Planck Institute for Human Cognitive and Brain Sciences.

Slagter HA, Giesbrecht B, Kok A, Weissman DH, Kenemans JL, Woldorff MG, Mangun GR. 2007. fMRI evidence for both generalized and specialized components of attentional control. Brain Res. 1177:90–102.

Spagna A, Mackie M-A, Fan J. 2015. Supramodal executive control of attention. Frontiers in Psychology. 6:1–14.

Sridharan D, Levitin DJ, Menon V. 2008. A critical role for the right fronto-insular cortex in switching between central-executive and default-mode networks. Proc Natl Acad Sci USA. 105:12569–12574.

Sterzer P, Kleinschmidt A. 2010. Anterior insula activations in perceptual paradigms: often observed but barely understood. Brain Struct Funct. 214:611–622.

Stoppel CM, Boehler CN, Strumpf H, Krebs RM, Heinze HJ, Hopf JM, Schoenfeld MA. 2013. Distinct representations of attentional control during voluntary and stimulus-driven shifts across objects and locations. Cereb Cortex. 23:1351–1361.

Tang Y-Y, Posner MI. 2014. Training brain networks and states. Trends Cogn Sci. 18:345–350.

Todd JJ, Fougnie D, Marois R. 2005. Visual short-term memory load suppresses temporo-parietal junction activity and induces inattentional blindness. Psychol Sci. 16: 965–972.

Tombu MN, Asplund CL, Dux PE, Godwin D, Martin JW, Marois R. 2011. A unified attentional bottleneck in the human brain. Proc Natl Acad Sci USA. 108:13426–13431.

Uddin LQ. 2015. Salience processing and insular cortical function and dysfunction. Nat Rev Neurosci. 16:55–61.

Van Essen DC, Drury HA, Dickson J, Harwell J, Hanlon D, Anderson CH. 2001. An integrated software suite for surface-based analyses of cerebral cortex. J Am Med Inform Assoc. 8:443–459.

van Steenbergen H, Band GPH, Hommel B, Rombouts SARB, Nieuwenhuis S. 2015. Hedonic hotspots regulate cingulate-driven adaptation to cognitive demands. Cereb Cortex. 25:1746–1756.

Voss A, Nagler M, Lerche V. 2013. Diffusion models in experimental psychology: a practical introduction. Exp Psychol. 60:385–402.

Wen X, Liu Y, Yao L, Ding M. 2013. Top-down regulation of default mode activity in spatial visual attention. J Neurosci. 33:6444–6453.

Wen X, Yao L, Liu Y, Ding M. 2012. Causal interactions in attention networks predict behavioral performance. J Neurosci. 32:1284–1292.

Woo C-W, Krishnan A, Wager TD. 2014. Cluster-extent based thresholding in fMRI analyses: pitfalls and recommendations. NeuroImage. 91:412–419.

Yeo B, Krienen F. 2011. The organization of the human cserebral cortex estimated by intrinsic functional connectivity. J Neurophysiol. 106:1125–1165.